Comparing occultation-derived sizes of TNOs with radiometric results

Mike Kretlow^{1,2}, Jose-Luis Ortiz¹, et al.

- (1) Instituto de Astrofísica de Andalucía (IAA), Granada, Spain
- (2) Deutsches Zentrum für Astrophysik (DZA), Görlitz, Germany

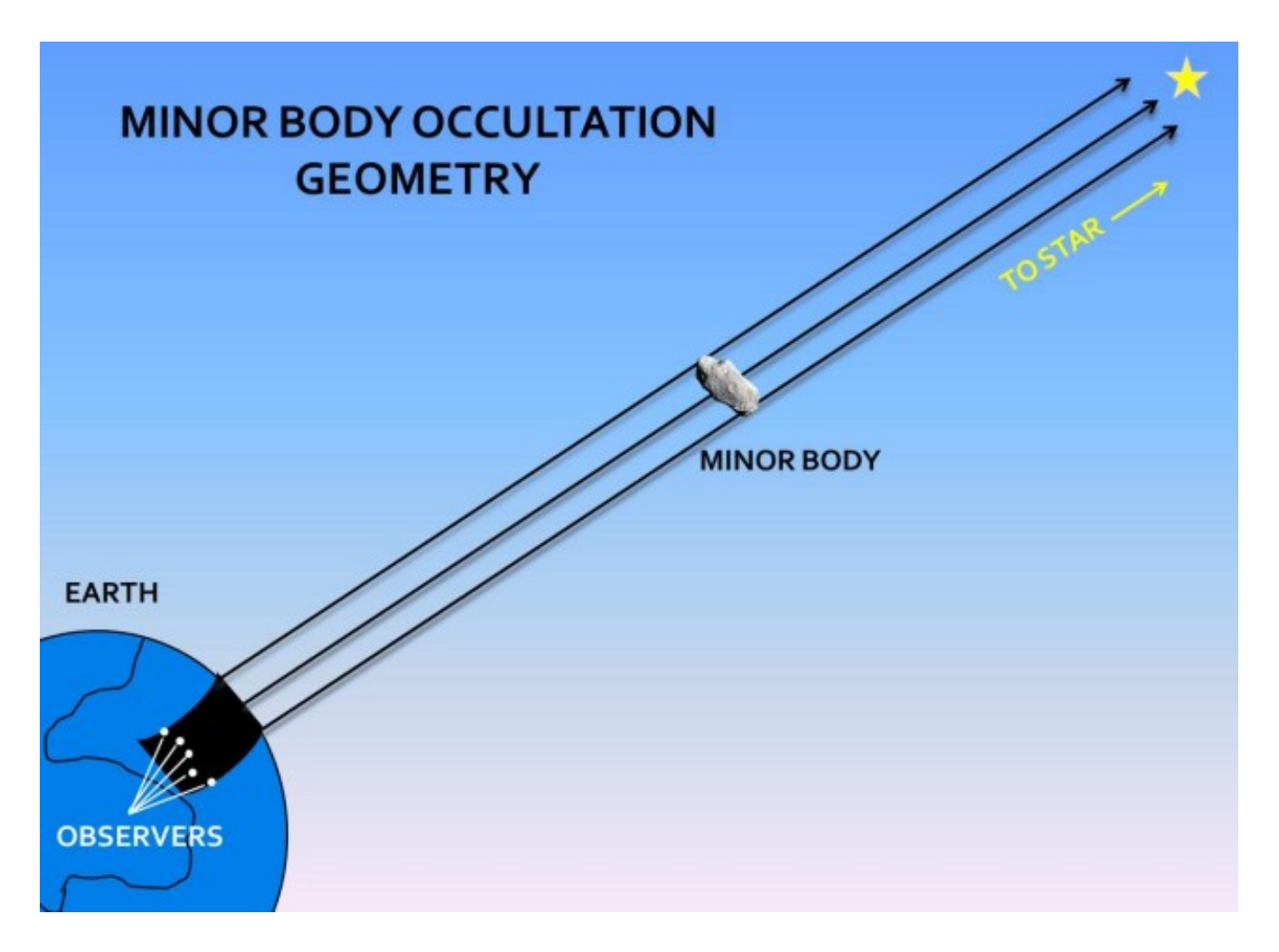
44th European Symposium on Occultation Projects Poznań, Poland, 23 – 24 August 2025

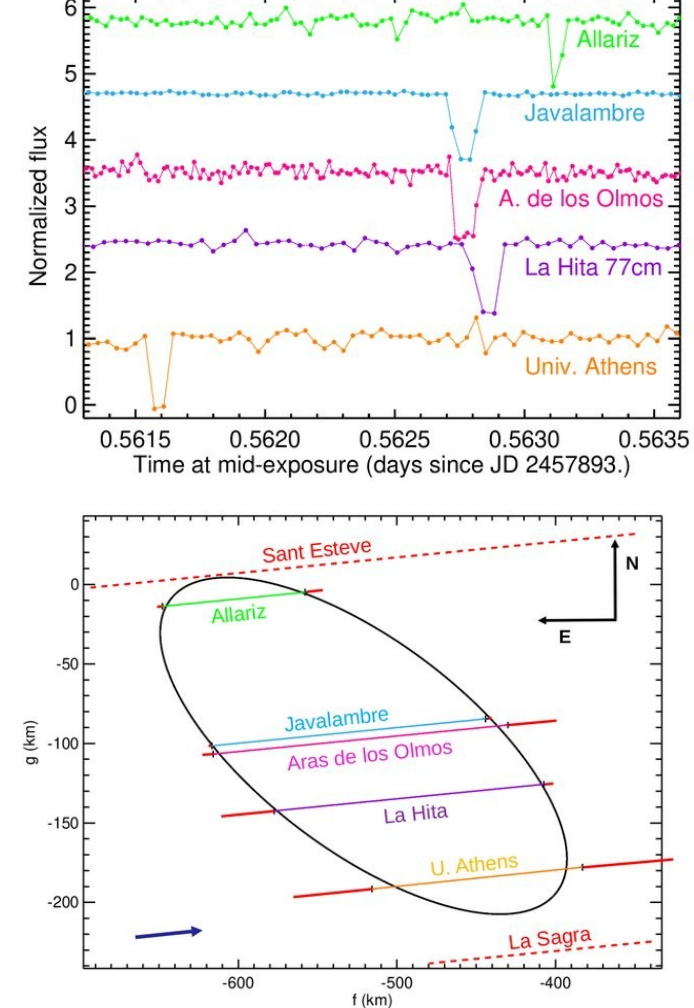




Motivation

- Trans-Neptunian objects (TNOs) are key to understanding the outer Solar System's formation and evolution.
- Size and albedo are fundamental physical properties for characterizing trans-Neptunian objects and Centaurs.
- Because these objects are distant and faint, they are challenging to observe.
- Thermal observations from the Herschel, Spitzer, and WISE space telescopes have yielded size and albedo estimates for approximately 180 TNOs and Centaurs. The majority of these, around 130 objects, were observed as part of the Herschel "TNOs are Cool" program.
- With an increasing number of successful observed stellar occultations we are now able to systematically compare the results provided by both techniques in order to benchmark the radiometric derived sizes.





Credit: IOTA

Thermal models

STM and NEATM

Simplification:

- spherical, equilibrium etc.
- surfaces

Restrictions / errors sources:

- simplifications
- satellite contribution
- beaming factor η (empirical)
- highly oblated shapes

Thermophysical models

- needs spin information
- +...

Spitzer 2003-<mark>2020</mark>



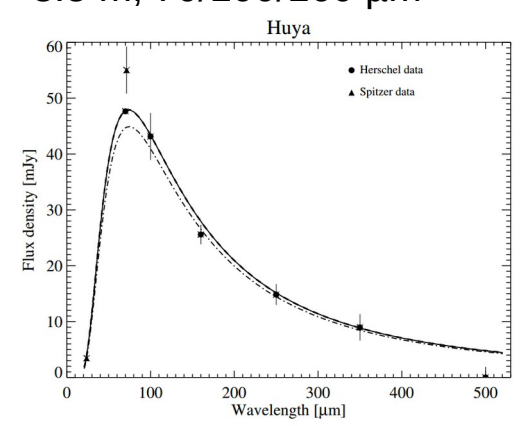
85 cm, 24/70/160 μm

TNOs: Avg. surface temp. ~35 K Peak wavelength 83 µm

Herschel 2009-2013



3.5 m, 70/100/160 µm



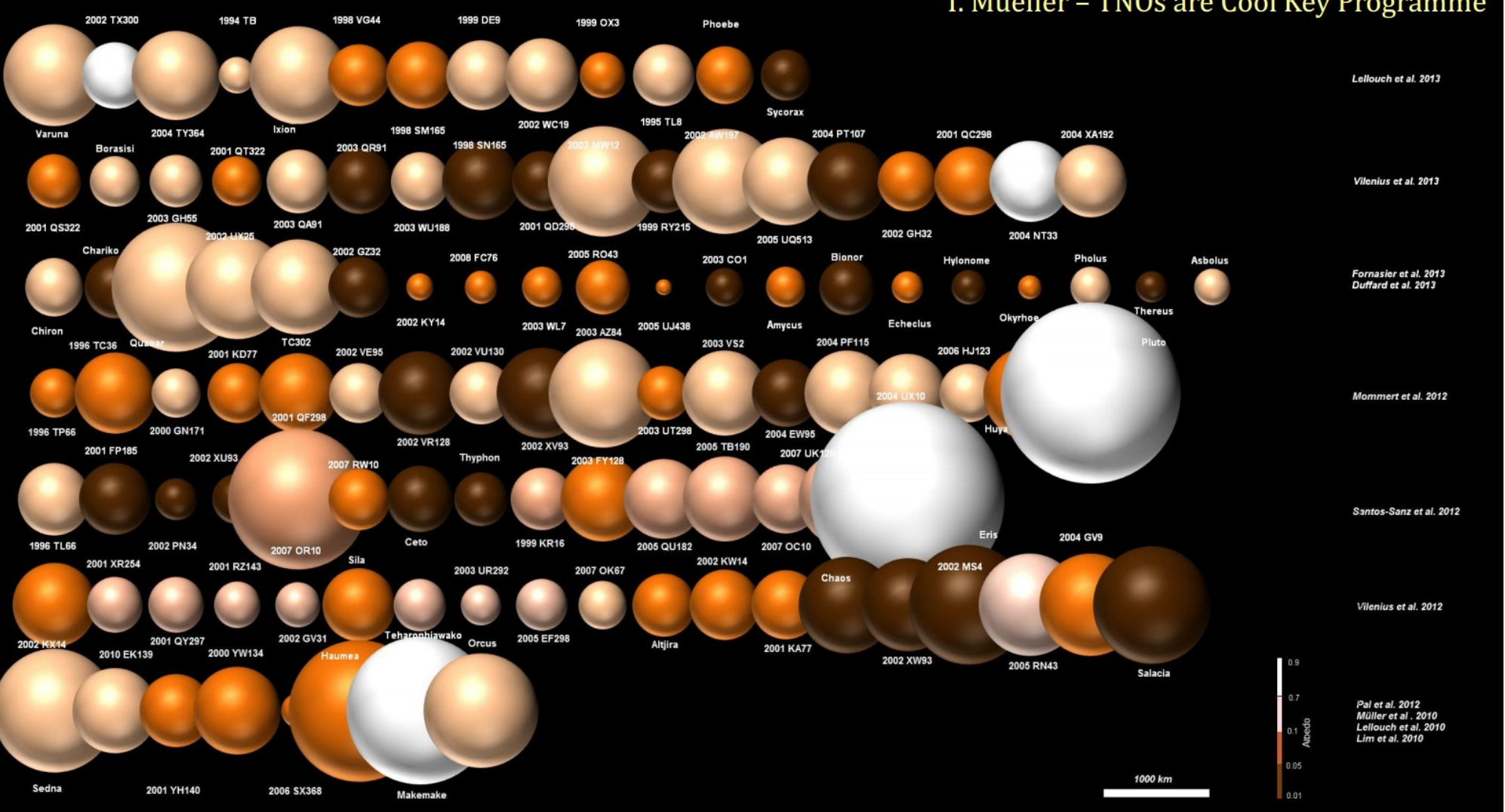
Herschel key program



~ 130 TNOs > 20 paper

No new data in near future (except JWST)

T. Mueller – TNOs are Cool Key Programme



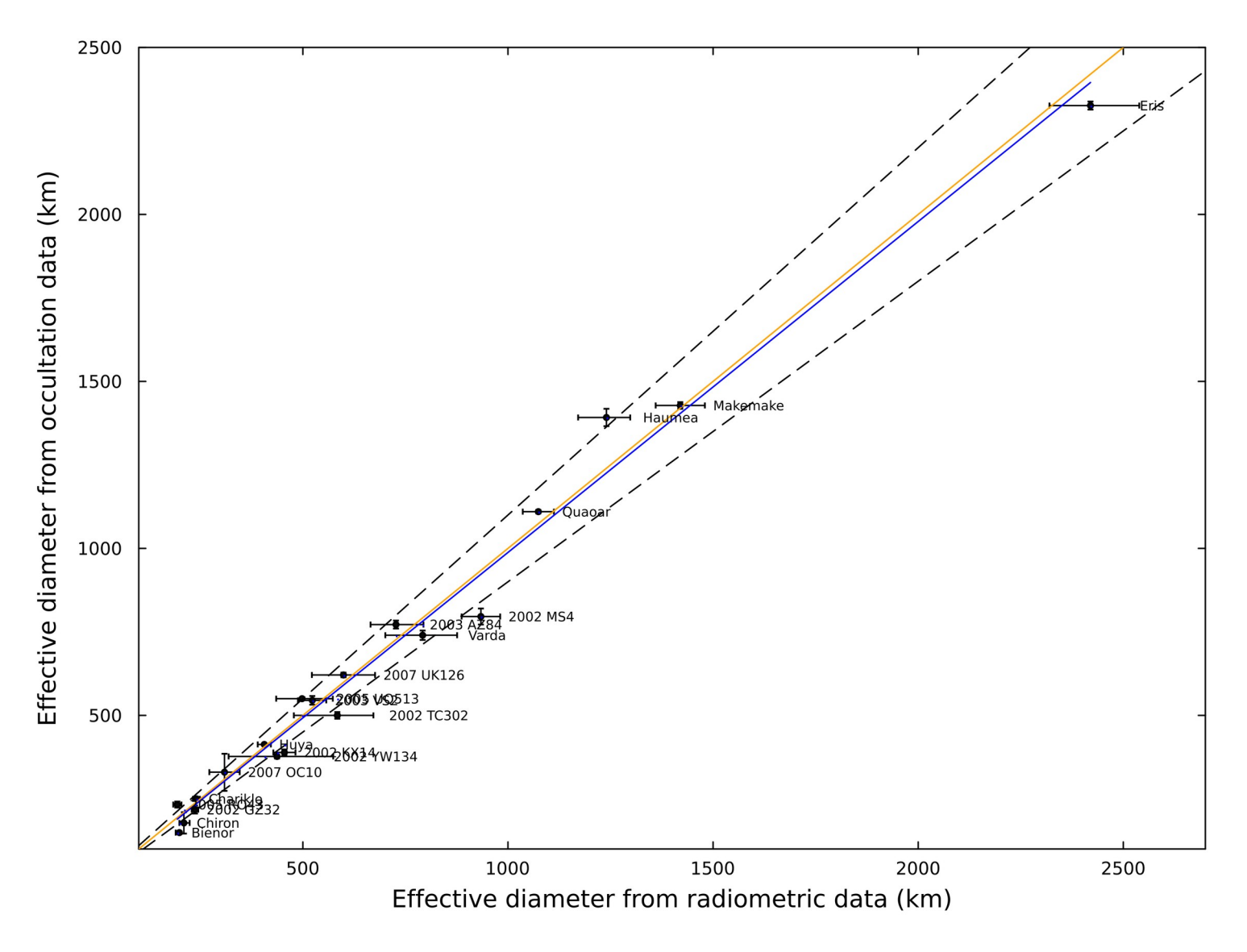
Object	DC	SR	D (ThM)	D (Occ)	H_V (ThM)	p_V (ThM)	p_V (Occ)	p_V^* (Occ)
Eris	SDO	S	2420 ⁺¹⁰⁰ ₋₁₁₉	2326 ± 12	-1.12 ± 0.03	86.7+9.8	96+9	91.7 ± 2.7
Haumea	Hau	SR	1240^{+69}_{-58}	1392 ± 26	0.43 ± 0.01	80.4 + 6.2 - 9.5	51 ± 2	61.4 ± 2.4
Huya	Plu	S	406 ± 16	413 ± 0.3	5.04 ± 0.03	8.3 ± 0.4	7.8 ± 0.2	10.0 ± 0.3
Makemake	Cub	S	1420 ± 60	1428 ± 10	0.14 ± 0.05	84 ± 6	81 - 5	76.3 ± 3.7
Quaoar	Cub	SR	1074 ± 38	1110 ± 5	2.73 ± 0.06	12.7 ± 1	7.9 ± 0.4	11.6 ± 0.7
Varda	Cub	S	792^{+91}_{-84}	740 ± 14	3.61 ± 0.05	$10.2^{+2.4}_{-2.0}$	9.9 ± 0.2	11.6 ± 0.7
2002 KX14	TNO		455 ± 27	389 ± 9	4.86 ± 0.10	$9.7^{+1.4}_{-1.3}$	11.9 ± 0.7	13.3 ± 1.4
2002 MS4	Cub		934 ± 47	796 ± 24	4.0 ± 0.6	$5.1^{+3.6}_{-2.2}$	10.0 ± 2.5	7.0 ± 3.9
2002 TC302	2:5		$584^{+106}_{-88.0}$	500 ± 10	4.17 ± 0.10	$11.5^{+4.7}_{-3.3}$	14.7 ± 0.5	15.2 ± 1.5
2002 YW134	3:8	S	437^{+118}_{-137}	377 ± 6	4.65 ± 0.06	13.3+17.3	17.2 ± 1.1	17.2 ± 1.1
2003 AZ84	Plu	S	727+62	772 ± 12	3.74 ± 0.08	10.7+2.3	$9.7^{+0.9}_{-0.9}$	9.5 ± 0.8
2003 VS2	Plu		523 ⁺³⁵ ₋₃₄	545 ± 13	4.11 ± 0.38	14.7+6.3	13.4 ± 1.0	13.6 ± 4.8
2005 UQ513	Cub		498+63	$550 \pm na$	3.87 ± 0.14	20.2+8.4	16.6 ± 2.1	16.6 ± 2.1
2007 OC10	SDO		309 ± 37	330 ⁺⁵⁶ ₋₅₅	5.43 ± 0.10	12.7+4.0	11.2 ^{+2.1} _{-5.0}	10.9 ± 2.6
2007 UK126	SDO	S	599 ± 77	621 ± 7	3.69 ± 0.10	16.7+5.8	15.0 ± 1.6	15.3 ± 1.5
Bienor	Cen		199+9	149 ± 4	7.57 ± 0.34	$4.1^{+1.6}_{-1.2}$	6.5 ± 0.5	7.6 ± 2.4
Chariklo	Cen	R	241^{+9}_{-8}	250 ^{+6.0} _{-4.6}	7.30 ± 0.20	$3.7^{+0.9}_{-0.8}$	_	3.4 ± 0.6
Chiron	Cen	R	210^{+11}_{-14}	178 ± 32	5.92 ± 0.20	17.2+4.3	7.6 ± 2.6	23.9 ± 9.7
2002 GZ32	Cen		237 ± 8	218 ± 12	7.37 ± 0.10	3.7 ± 0.4	4.3 ± 0.7	4.2 ± 0.6
2005 RO43	Cen		194 ± 10	233 ± 9	7.34 ± 0.51	$5.6^{+3.6}_{-2.1}$	3.8 ± 1.8	3.8 ± 1.8

References

Altenhoff et al. (2001). Bauer et al. (2013). Benedetti-Rossi et al. (2016), Benedetti-Rossi et al. (2019), Braga-Ribas et al. (2013), Braga-Ribas et al. (2014), Braga-Ribas et al. (2023), Brown (2013), Brown and Truiillo (2004), Brucker et al. (2009), Bus et al. (1996), Dias-Oliveira et al. (2017), Duffard et al. (2014), Farkas-Takács et al. (2020), Fernández-Valenzuela et al. (2023), Fornasier et al. (2013), Fraser and Brown (2010), Gómez-Limón et al. (2025), Groussin et al. (2004), Groussin et al. (2004), Grundy et al. (2015). Jewitt and Kalas (1998). Kiss et al. (2024), Kretlow et al. (2021), Kretlow et al. (2022), Kretlow (2025, in prep.), Leiva et al. (2017), Lellouch et al. (2010), Lellouch et al. (2013), Lellouch et al. (2017), Lim et al. (2010), Mommert et al. (2012), Morgado et al. (2021), Ortiz et al. (2012), Ortiz et al. (2017), Ortiz et al. (2020), Pereira et al. (2023), Rizos et al. (2024), Rizos et al. (2025), Rommel et al. (2023), Rommel et al. (2025), Santos-Sanz et al. (2012), Santos-Sanz et al. (2021), Santos-Sanz et al. (2022), Schindler et al. (2017), Sicardy et al. (2011), Sickafoose et al. (2020), Souami et al. (2020), Stansberry et al. (2008), Vara-Lubiano et al. (2022), Vilenius et al. (2012), Vilenius et al. (2014), Santos-Sanz et al. (2012)

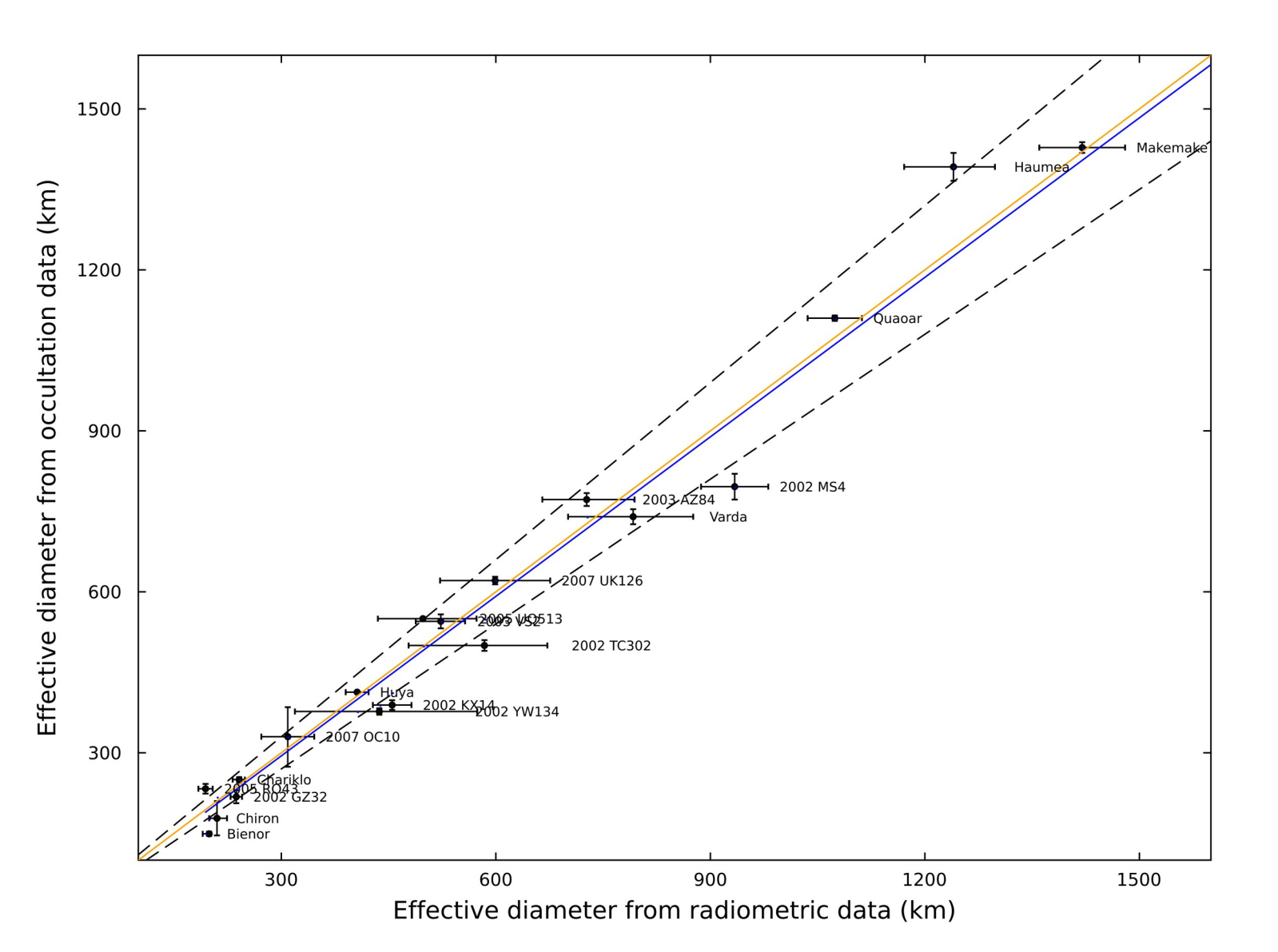
15 TNOs, 5 Centaurs

⁺ unpublished work



Comparison between effective diameters obtained using the radiometric technique (D_{rad} , x-axis) and those obtained from stellar occultations (D_{occ} , y-axis)

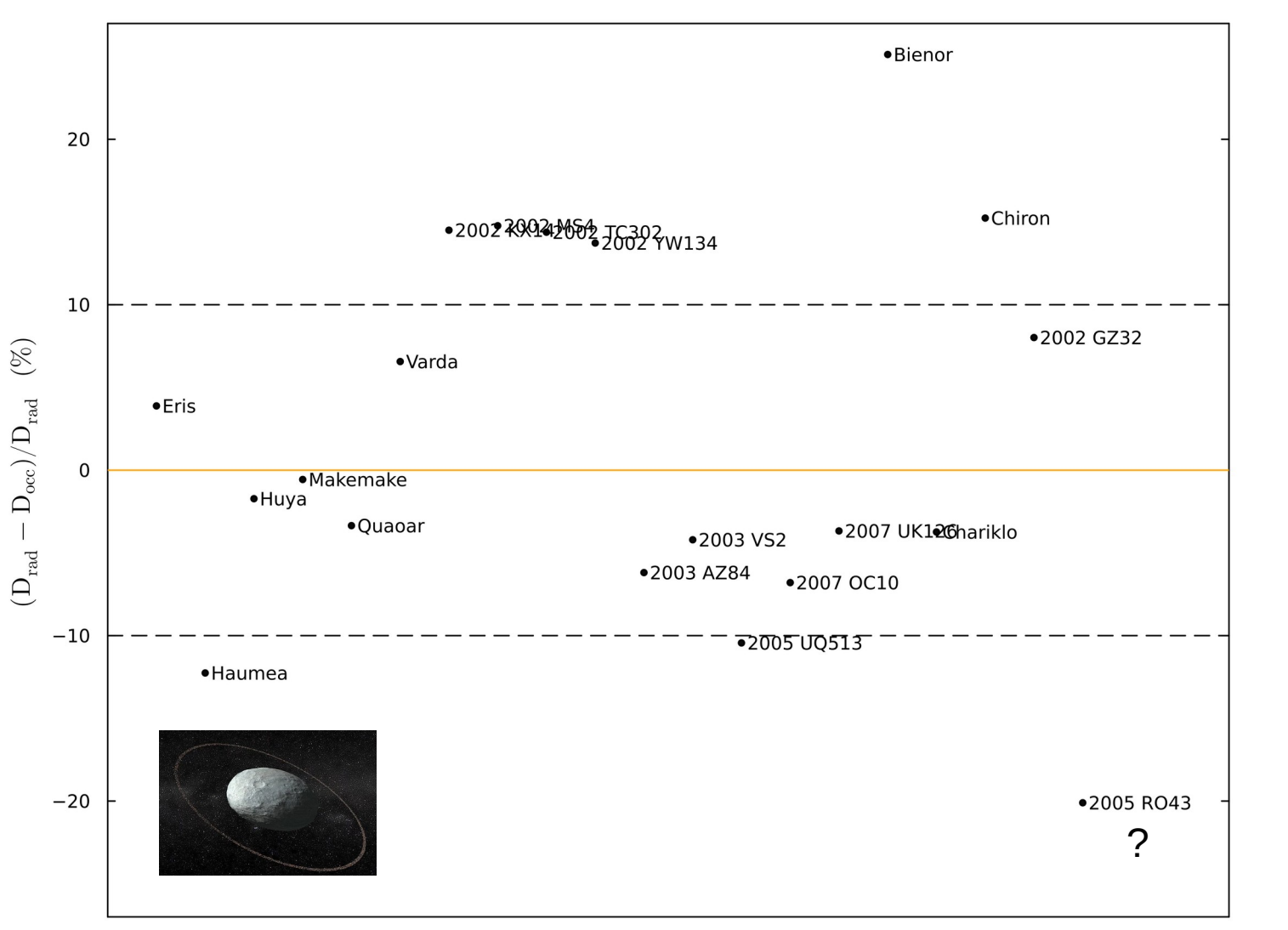
Orange line: y=x Blue line: linear fit



Occultation-derived (effective) diameters (D_{occ}) vs radiometric (effective) diameters (D_{rad}).

Close-up of previous figure.

Orange line: y=x Blue line: linear fit



Relative differences between radiometric and occultation diameters, $(D_{rad} - D_{occ})/D_{rad}$

The dashed lines indicate a ±10% relative deviation in diameter

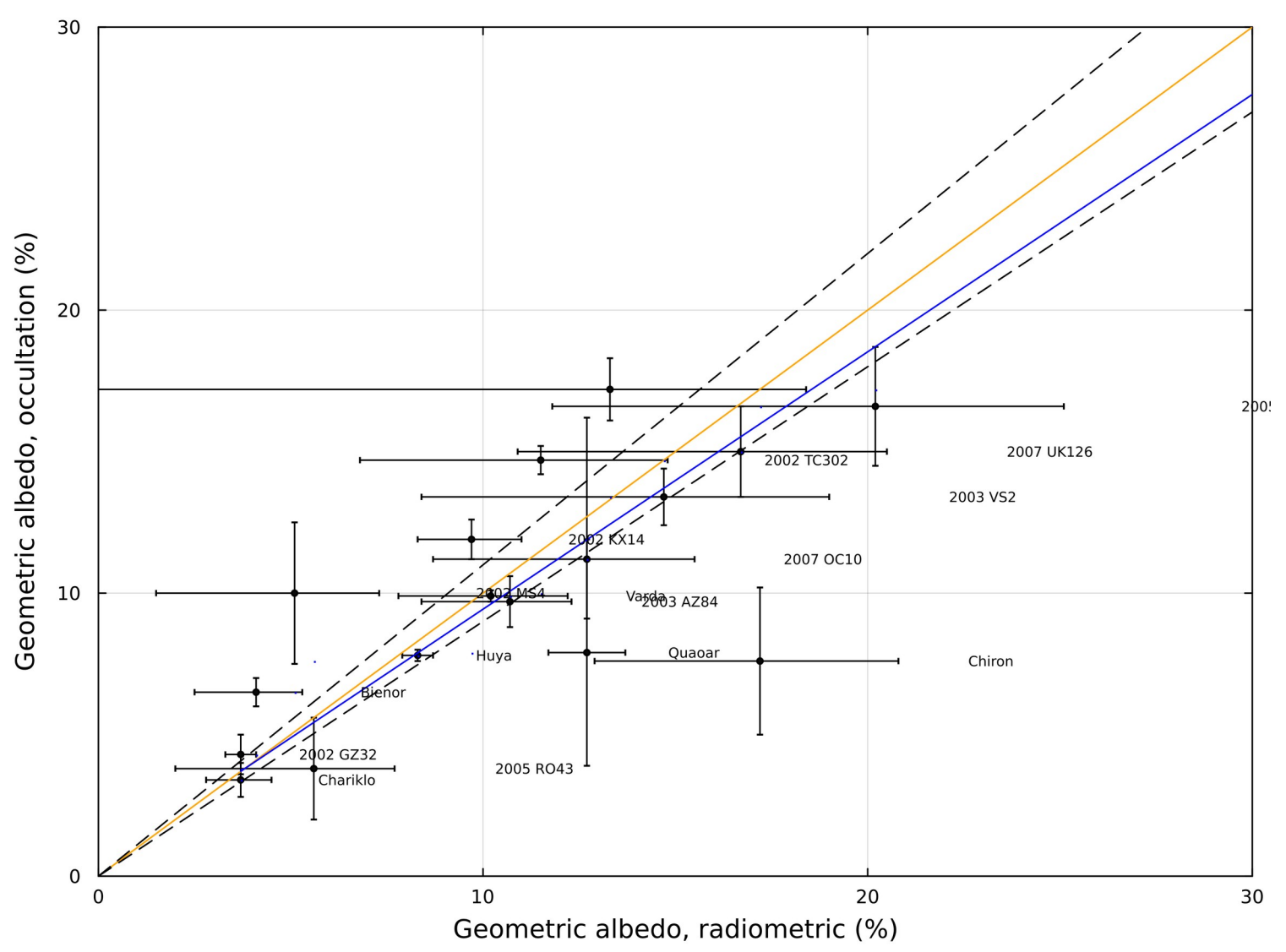
Orange line: y=x Blue line: linear fit

Metric: mean weighted normalized orthogonal distance (MWNOD)

$$\langle d_{\perp} \rangle = \frac{1}{N} \sum_{i=1}^{N} \frac{\left| D_{\text{rad},i} - D_{\text{occ},i} \right|}{\sqrt{\sigma_{\text{rad},i}^2 + \sigma_{\text{occ},i}^2}} .$$
 $\langle d_{\perp} \rangle = 11.8\%$

If occultation diameters are considered exact, this value suggest an average uncertainty for radiometric diameters in the range of $\sim 10\% - 15\%$.

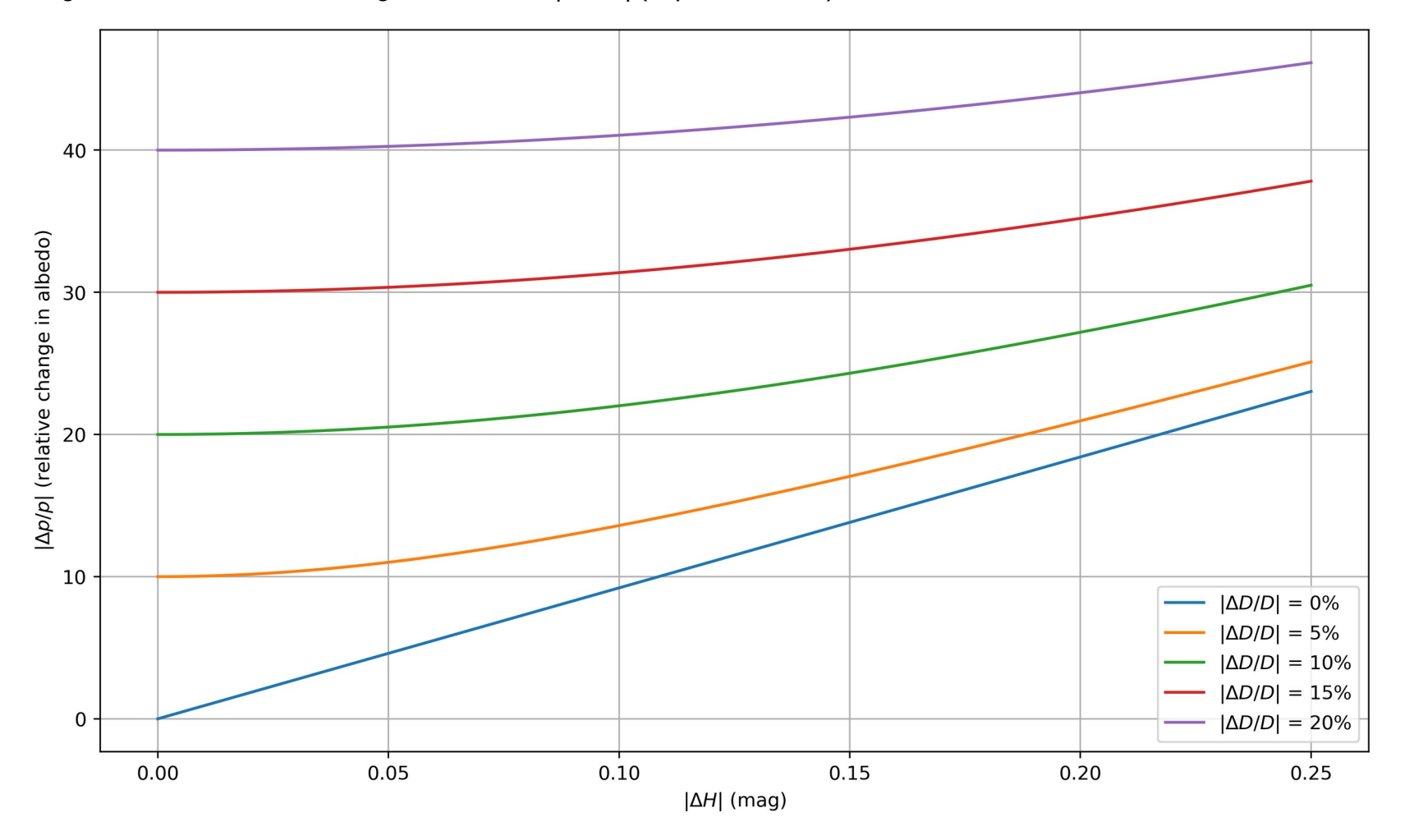
This observation is in agreement with previous findings for thermally derived diameters of asteroids from AKARI, IRAS, and WISE/NEOWISE.



Comparison of geometric albedos derived from radiometry (p_{rad}) and stellar occultation data (p_{occ}).

Orange line: y=x Blue line: linear fit

Propagation of uncertainty in albedo: the magnitude of the relative change in geometric albedo, $|\Delta p/p|$ (expressed in %), plotted against the magnitude of the change in absolute magnitude, $|\Delta H|$ (in mag). Each curve illustrates a different fixed magnitude of the relative change in diameter, $|\Delta D/D|$ (expressed in %).



Conclusions

- Stellar occultation and radiometric methods show good overall agreement in diameter estimates, with a mean weighted normalized orthogonal distance (MWNOD) of 11.8%.
- Simple thermal models (NEATM), despite lacking corrections for multiplicity or non-sphericity, are sufficient to produce consistent diameters in most cases.
- Outliers with $(D_{rad} D_{occ})/D_{rad} \gtrsim +(10 12)\%$ may be linked to unresolved companions and/or ring systems contributing excess thermal flux.
- Significant radiometric underestimates, as seen for Haumea and 2005 RO43, highlight cases where thermal models may fall short, particularly for complex or highly elongated objects.

Conclusions

- Uncertainties in absolute magnitude H are a major source of error in geometric albedo determination, significantly affecting thermal model results and contributing to discrepancies between methods.
- Reliable albedo comparisons between techniques require consistent and accurate H values, highlighting the need for standardized and contemporaneous photometric measurements.

Stellar occultations remain a critical tool for validating and refining thermal models, especially for non-spherical or complex bodies.

Extra Slides